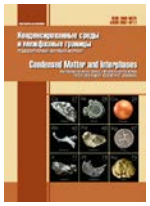

ISSN 1606-867X (Print)
ISSN 2687-0711 (Online)
Condensed Matter and Interphases
Kondensirovannye Sredy i Mezhfaznye Granitsy
https://journals.vsu.ru/kcmf/

Original articles

Research article
https://doi.org/10.17308/kcmf.2021.23/3527

Double molybdates of silver and monovalent metals

T. S. Spiridonova[1]✉, S. F. Solodovnikov[2], Yu. M. Kadyrova[1,3], Z. A. Solodovnikova[2], A. A. Savina[1,4], E. G. Khaikina[1,3]

[1]Baikal Institute of Nature Management, Siberian Branch of the Russian Academy of Sciences, 6 ulitsa Sakhyanovoy, Ulan-Ude, Republic of Buryatia 670047, Russian Federation

[2]Nikolaev Institute of Inorganic Chemistry, Siberian Branch of the Russian Academy of Sciences, 3 Akademika Lavrentieva prospekt, Novosibirsk 630090, Russian Federation

[3]Banzarov Buryat State University, 24a ulitsa Smolina, Ulan-Ude, Republic of Buryatia 670000, Russian Federation

[4]Skolkovo Institute of Science and Technology, 30, bld. 1 Bolshoy Boulevard, Moscow 121205, Russian Federation

Abstract

The Ag_2MoO_4–Cs_2MoO_4 system was studied by powder X-ray diffraction, the formation of a new double molybdate $CsAg_3(MoO_4)_2$ was established, its single crystals were obtained, and its structure was determined. $CsAg_3(MoO_4)_2$ (sp. gr. $P\bar{3}$, $Z = 1$, $a = 5.9718(5)$, $c = 7.6451(3)$ Å, $R = 0.0149$) was found to have the structure type of $Ag_2BaMn(VO_4)_2$. The structure is based on glaserite-like layers of alternating MoO_4 tetrahedra and $Ag1O_6$ octahedra linked by oxygen vertices, which are connected into a whole 3D framework by $Ag2O_4$ tetrahedra. An unusual feature of the Ag2 atom environment is its location almost in the centre of an oxygen face of the $Ag2O_4$ tetrahedron. Caesium atoms are in cuboctahedral coordination (CN = 12).

We determined the structures of the double molybdate of rubidium and silver obtained by us previously and a crystal from the solid solution based on the hexagonal modification of Tl_2MoO_4, which both are isostructural to glaserite $K_3Na(SO_4)_2$ (sp. gr. $P\bar{3}m1$). According to X-ray structural analysis data, both crystals have nonstoichiometric compositions $Rb_{2.81}Ag_{1.19}(MoO_4)_2$ ($a = 6.1541(2)$, $c = 7.9267(5)$ Å, $R = 0.0263$) and $Tl_{3.14}Ag_{0.86}(MoO_4)_2$ ($a = 6.0977(3)$, $c = 7.8600(7)$ Å, $R = 0.0174$). In the case of the rubidium compound, the splitting of the Rb/Ag position was revealed for the first time among molybdates. Both structures are based on layers of alternating MoO_4 tetrahedra and AgO_6 or (Ag, Tl)O_6 octahedra linked by oxygen vertices. The coordination numbers of rubidium and thallium are 12 and 10.

Keywords: Double molybdates, Silver, Monovalent metals, Binary systems, X-ray diffraction study, Structure, Glaserite

Acknowledgements: the authors are grateful to PhD Irina A. Prodan (Gudkova) and Ms Oksana A. Gulyaeva for recording and processing the X-ray diffraction data of the crystals on a Bruker X8 Apex CCD automated diffractometer. This research was supported by the Ministry of Science and Higher Education of the Russian Federation, projects No. 0273-2021-0008 (Baikal Institute of Nature Management, SB RAS), and No. 121031700313-8 (Nikolaev Institute of Inorganic Chemistry, SB RAS).

For citation: Spiridonova T. S., Solodovnikov S. F., Kadyrova Yu. M., Solodovnikova Z. A., Savina A. A., Khaikina E. G. Double molybdates of silver and monovalent metals. *Kondensirovannye sredy i mezhfaznye granitsy = Condensed Matter and Interphases*. 2021;23(3): 421–431. https://doi.org/10.17308/kcmf.2021.23/3527

Для цитирования: Спиридонова Т. С., Солодовников С. Ф., Кадырова Ю. М., Солодовникова З. А., Савина А. А., Хайкина Е. Г. Двойные молибдаты серебра и одновалентных металлов. *Конденсированные среды и межфазные границы*. 2021;23(3): 421–431. https://doi.org/10.17308/kcmf.2021.23/3527

✉ Tatyana S. Spiridonova, e-mail: spiridonova-25@mail.ru

1. Introduction

Double molybdates of alkaline elements with divalent and trivalent metals are well known as promising phosphors [1–6], ferroelectrics and ferroelastics [7–9], solid electrolytes [10–13], electrode [14–19], laser [20–24], and other materials. A prominent place in the series of double molybdates is also occupied by phases formed in the M_2MoO_4–M'_2MoO_4 systems (M, M' – alkaline elements). The largest number of publications is devoted to M_2MoO_4–Li_2MoO_4 (M = K, Rb, Cs) systems and the double molybdates MLiMoO$_4$ formed in them. The compounds melt congruently and have developed polymorphism, and ferroelectric and ferroelastic properties [25–32]. Based on the results of studying the Na_2MoO_4–Li_2MoO_4 system by visual polythermic method, differential thermal analysis and X-ray powder diffraction, it was concluded in [25, 33, 34] that there are the phases with compositions 3:1 and 6:1 in the system; however, both compounds were not isolated and characterised. In the systems M_2MoO_4–Na_2MoO_4 (M = K, Rb, Cs), double molybdates $M_{2-x}Na_xMoO_4$ (M = K, Rb, Cs) were found [33, 35–39], which crystallize in the structure type of glaserite $K_3Na(SO_4)_2$ [40]. Unlike stoichiometric $Cs_3Na(MoO_4)_2$ [39], in the systems M_2MoO_4–Na_2MoO_4 (M = K, Rb) the glaserite-type phases have upper temperature limits of stability and noticeable homogeneity ranges: $K_{2-x}Na_xMoO_4$ ($0.40 \leqslant x \leqslant 1.0$) [36] and $Rb_{2-x}Na_xMoO_4$ ($0.50 \leqslant x \leqslant 0.67$) [37]. Another compound $RbNa_3(MoO_4)_2$ revealed in the Rb_2MoO_4–Na_2MoO_4 system is unstable at room temperature [37].

Until now, data on double molybdates of silver and monovalent metals were absent, although studies of the corresponding binary systems were undertaken. Thus, according to [41, 42], in the Ag_2MoO_4–Li_2MoO_4 system intermediate phases are not formed, while the authors of [43] on the base of the results of a visual polythermic analysis of the Ag_2MoO_4–Na_2MoO_4 system made a conclusion about formation of a continuous series of solid solutions with a minimum. The formation of continuous solid solutions of the spinel type was also confirmed by X-ray diffraction studies of the latter system [44]. One of the compositions of this solid solution ($NaAgMoO_4$) was studied in [45, 46]. The formation of boundary solid solutions was reported for the Ag_2MoO_4–Tl_2MoO_4 system [47, 48].

The first double molybdate of silver and an alkali metal was obtained by us when studying the Ag_2MoO_4–Rb_2MoO_4 system. The compound $Rb_3Ag(MoO_4)_2$ melts at 435 °C and has a glaserite structure type [49]. Later, in the similar potassium containing system, we obtained a hexagonal double molybdate, $K_{7-x}Ag_{1+x}(MoO_4)_4$ ($0 \leqslant x \leqslant 0.4$) [50], which crystallizes in its own structure type and at 334 °C undergoes a reversible first-order phase transition from the acentric form (sp. gr. $P6_3mc$) into centrosymmetric one.

In this study, we investigated the Ag_2MoO_4–Cs_2MoO_4 system and determined the crystal structure of the compound formed in it. In addition, the structure of double rubidium-silver molybdate was refined and an X-ray diffraction analysis of one of the members of the solid solution formed in the Ag_2MoO_4–Tl_2MoO_4 system on the base of the high-temperature modification of thallium molybdate [51] was performed.

2. Experimental

Commercially available $AgNO_3$, $TlNO_3$ (analytical reagent grade), MoO_3 (chemically pure grade), Cs_2CO_3 (extra-pure grade) reagents were used as starting materials. M_2MoO_4 (M = Ag, Tl) was obtained by calcining stoichiometric amounts of MNO$_3$ and MoO_3 with gradually increasing temperatures from 300–350 to 450 °C (in the case of silver) and up to 500 °C (in the case of thallium) for 50 h. Caesium molybdate was synthesised by the reaction $Cs_2CO_3 + MoO_3 = Cs_2MoO_4 + CO_2$ with annealing at 450–550 °C for 80 h. The thermal and crystallographic characteristics of the obtained compounds agreed with the literature data.

Powder X-ray diffraction (PXRD) analysis was carried out using a Bruker D8 ADVANCE automated powder diffractometer ($\lambda Cu K_\alpha$, secondary monochromator, scanning step $2\theta = 0.02076°$).

X-ray single crystal diffraction data for crystal structure determinations were taken at room temperature using Bruker-Nonius X8 Apex automated diffractometer with a two-dimensional CCD detector (MoK_α-radiation, graphite monochromator, φ-scanning with a scanning interval of 0.5°) in the hemisphere of reciprocal space. Calculations for solving and refinement of the structures were performed using the SHELX-97 software package [52].

3. Results and discussion

3.1. Cs_2MoO_4–Ag_2MoO_4 system and crystal structure of $CsAg_3(MoO_4)_2$

The Cs_2MoO_4–Ag_2MoO_4 system was studied by PXRD in the subsolidus region in the entire concentration range with a step of 5–10 mol% (2.5 mol% in some cases). The formation of an intermediate compound $CsAg_3(MoO_4)_2$ was established (the composition was found by single crystal structure determination). According to PXRD data, the formation of this compound begins at 300 °C; however, a single-phase $CsAg_3(MoO_4)_2$ sample was not obtained. An increase of the duration of reaction mixtures calcination (up to 500 h), an expansion of the temperature range (up to the limits of subsolidus temperatures), as well as the use of stoichiometric $AgNO_3$, Cs_2MoO_4, MoO_3 or Ag_2MoO_4, Cs_2CO_3, MoO_3 mixtures as starting components instead of simple silver and caesium molybdates, did not lead to a positive result.

Single crystals of $CsAg_3(MoO_4)_2$ suitable for X-ray structural analysis were obtained by spontaneous crystallization of the melt of a sintered sample of the compound, which was heated to 470 °C, kept at this temperature for 30 min and cooled at a rate of 4°/h down to 200 °C (then in a switched-off and cooling further). Crystal data and the structure refinement results are given in Table 1, the atomic coordinates and interatomic distances are listed in Tables 2 and 3.

The structure of $CsAg_3(MoO_4)_2$ was solved in the trigonal sp. gr. $P\bar{3}$ and it was found to be isostructural to $Ag_2BaMn(VO_4)_2$ [53]. The Mo atoms and 2/3 silver atoms (the Ag2 position) were tetrahedrally coordinated with the Mo–O distances 1.743(4)–1.776(2) Å, Ag2–O 2.314(2)–2.499(4) Å. An unusual feature of the Ag2 environment is its location almost in the centre of the oxygen face of $Ag2O_4$ tetrahedron (Fig. 1), which was also found in the $K_{6.68}Ag_{1.32}(MoO_4)_4$ structure [50]. The remaining third of silver atoms (Ag1) are located in octahedra with equal Ag1–O bond lengths of 2.446 (2) Å. The structure is based on glaserite-like layers of alternating MoO_4-tetrahedra and $Ag1O_6$-octahedra, which are linked by oxygen vertices and interconnected in a whole three-dimensional framework by $Ag2O_4$ tetrahedra (Fig. 1). The negative charge of the framework is compensated by caesium cations in cuboctahedral coordination (CN = 12); the Cs–O distances are 3.182(7)–3.451(1) Å.

3.2. Crystal structure of $Rb_{2.81}Ag_{1.19}(MoO_4)_2$

As we showed in [49], $Rb_3Ag(MoO_4)_2$ is the only intermediate compound of the Rb_2MoO_4–Ag_2MoO_4 system. A single-phase sample of the double rubidium-silver molybdate was synthesised by

Table 1. X-ray structure analysis data for $CsAg_3(MoO_4)_2$

Formula	$CsAg_3(MoO_4)_2$
Formula weight (g/mol)	776.40
Crystal system	Trigonal
Space group	$P\bar{3}$
Unit cell dimensions	a = 5.9718(5) Å, c = 7.6451(3) Å
V (Å^3) / Z	236.115(12) / 1
Calculated density (g cm^{-3})	5.460
Crystal size (mm)	0.15 × 0.06 × 0.06
μ(MoK_α), mm^{-1}	12.502
θ range (°)	5.328–61.126
Miller index ranges	$-8 \leqslant h \leqslant 8$, $-7 \leqslant k \leqslant 8$, $-10 \leqslant l \leqslant 10$
Reflections collected/unique	3234 / 490 [R_{int} = 0.0265]
Number of variables/constraints	24 / 0
Goodness-of-fit on F^2 (GOF)	1.158
Extinction coefficient	0.0087(6)
Final R indices [$I > 2\sigma(I)$] R indices (all data)	$R(F)$ = 0.0149, $wR(F^2)$ = 0.0349 $R(F)$ = 0.0158, $wR(F^2)$ = 0.0353
Largest difference peak / hole (e Å^{-3})	0.81/–1.15

Таблица 2. Координаты и эквивалентные изотропные тепловые параметры атомов в структуре $CsAg_3(MoO_4)_2$

Atom	*x/a*	*y/b*	*z/c*	U_{eq}(Å²)*
Mo	0.6667	0.3333	0.25304(5)	0.01327(11)
Ag1	0	0	0	0.02048(11)
Ag2	0.3333	0.6667	0.19216	0.02805(13)
Cs	0	0	0.5	0.02047(12)
O1	0.6667	0.3333	0.4810(5)	0.0306(9)
O2	0.7014(4)	0.631(4)	0.1792(3)	0.0242(4)

* $U_{eq} = 4(U_{11} + U_{22} + 0.75U_{33} - U_{12}) / 9$.

Table 3. Selected interatomic distances **(Å) in** $CsAg_3(MoO_4)_2$

Mo-tetrahedron		Ag1-octahedron	
Mo1–O1	1.743(4)	Ag1–O2	2.446(2) × 6
–O2	1.776(2) × 3		
<Mo1–O>	1.768		
Cs-polyhedron		**Ag2-tetrahedron**	
Cs–O2′	3.181(2) × 6	Ag2–O2	2.314(2) × 3
–O1	3.4509(2) × 6	–O1	2.499(4)
<Cs–O>	3.316	<Ag2–O>	2.360

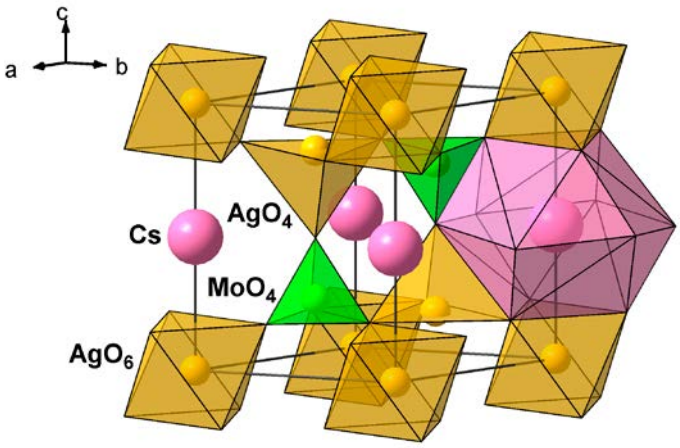

Fig. 1. Crystal structure of $CsAg_3(MoO_4)_2$

annealing a stoichiometric mixture of Ag_2MoO_4 and Rb_2MoO_4 at 380 °C for 100 h. Crystals suitable for X-ray structural analysis were obtained by spontaneous crystallisation from the melt. The preliminary results of X-ray structural analysis were previously published by us in [49]. In this study, the composition of the $Rb_{2.81}Ag_{1.19}(MoO_4)_2$ crystal and its structure were corrected and refined (Tables 4–6).

Note that the solid-state synthesis of a single-phase sample of the composition described above was not successful. After annealing the reaction mixtures of silver and rubidium molybdates, even at highest subsolidus temperatures, only $Rb_{3-x}Ag_{1+x}(MoO_4)_2$ ($0 \leqslant x \leqslant 0.10$) samples were single-phase. Probably, the found crystal composition has an extremely high silver content and can be obtained only from melts.

In the structure of $Rb_{2.81}Ag_{1.19}(MoO_4)_2$ (sp. gr. $P\bar{3}m1$) of the glaserite type $K_3Na(SO_4)_2$ [40], molybdenum atoms have tetrahedral oxygen coordination with the distances Mo–O 1.730(6)–1.773(3) Å. The Ag1 atoms are in octahedra with the equal bond lengths Ag–O 2.483(3) Å. The structure is based on layers of alternating MoO_4 tetrahedra and $Ag1O_6$ octahedra linked by

Table 4. X-ray structure analysis data for $Rb_{2.81}Ag_{1.19}(MoO_4)_2$ and $Tl_{3.14}Ag_{0.86}(MoO_4)_2$

Formula	$Rb_{2.81}Ag_{1.19}(MoO_4)_2$	$Tl_{3.14}Ag_{0.86}(MoO_4)_2$
Formula weight (g/mol)	688.42	1054.37
Crystal system	Trigonal	Trigonal
Space group	$P\bar{3}m1$	$P\bar{3}m1$
Unit cell dimensions	a = 6.1541(2) Å c = 7.9267(5) Å	a = 6.0977(3) Å c = 7.8600(7) Å
V (Å^3) / Z	259.99 (2) / 1	253.10 (3) / 1
Calculated density (g cm^{-3})	4.397	6.918
Crystal size (mm)	0.13 × 0.10 × 0.02	0.09 × 0.09 × 0.05
μ(MoK_α), mm^{-1}	3.645	53.840
θ range (°)	2.26–28.83	2.09–30.50
Miller index ranges	$-10 \leqslant h \leqslant 8$, $-10 \leqslant k \leqslant 7$, $-13 \leqslant l \leqslant 9$	$-5 \leqslant h \leqslant 8$, $-8 \leqslant k \leqslant 6$, $-11 \leqslant l \leqslant 10$
Reflections collected/unique	2370 / 504 [R_{int} = 0.0299]	2306 / 330 [R_{int} = 0.0314]
Number of variables/constraints	25 / 0	22 / 0
Goodness-of-fit on F^2 (GOF)	1.271	1.087
Extinction coefficient	0.0016 (3)	0.0035 (4)
Final R indices [$I > 2\sigma(I)$] R indices (all data)	$R(F)$ = 0.0263 $wR(F^2)$ = 0.0625 $R(F)$ = 0.0272 $wR(F^2)$ = 0.0627	$R(F)$ = 0.0174 $wR(F^2)$ = 0.0419 $R(F)$ = 0.0189 $wR(F^2)$ = 0.0425
Largest difference peak/hole (e Å^{-3})	1.00 / −1.21	0.87 / −0.87

Table 5. Coordinates and equivalent isotropic thermal parameters of atoms in the structure of $Rb_{2.81}Ag_{1.19}(MoO_4)_2$

Atom	Occ.	x/a	y/b	z/c	U_{eq} (Å^2)*
Mo	1	0.6667	0.3333	0.25304(5)	0.0149(2)
Ag1	1	0	0	0	0.0221(2)
Ag2	0.10(1)	0.3333	0.6667	0.179(5)	0.047(7)
Rb1	0.90(1)	0.3333	0.6667	0.1580(3)	0.0205(4)
Rb2	1	0	0	0.5	0.0296(3)
O1	1	0.6667	0.3333	0.4810(5)	0.055(2)
O2	1	0.7014(4)	0.631(4)	0.1792(3)	0.0321(7)

*$U_{eq} = 4(U_{11} + U_{22} + 0.75U_{33} - U_{12}) / 9$.

Table 6. Main interatomic distances (Å) in the structure of $Rb_{2.81}Ag_{1.19}(MoO_4)_2$

Mo-tetrahedron		Rb1-polyhedron	
Mo–O1	1.730(6)	Rb1–O1	2.705(7)
–O2	1.773(3) × 3	–O2	3.0990(5) × 6
		–O2′	3.296(4) × 3
<Mo–O>	1.762	<Rb1–O>	3.119
Ag1-octahedron		Rb2-polyhedron	
Ag1–O2	2.483(3) × 6	Rb2–O2	3.033(4) × 6
Ag2-polyhedron		–O1	3.5531(1) × 6
Ag2–O1	2.54(4)	<Rb2–O>	3.293
–O2	3.085(2) × 6		
<Ag2–O>	3.007		

common oxygen vertices (Fig. 2). The negative charge of the layers is compensated by two types of rubidium cations (CN = 12 and 10); the total range of Rb–O distances is 2.706(7) –3.553(1) Å. An additional position of silver (Ag2) near the Rb1 position (CN = 10) at the distance Rb1–Ag2 0.17(4) Å was found, which partially replaces rubidium in Rb1; the Ag2–O bond lengths are 2.54(4)–3.085(2) Å (CN = 7).

Splitting of the Rb/Ag position in molybdates was revealed for the first time. As for tungstates, it was found earlier in the structure $Ag_{3+x}Rb_{9-x}Sc_2(WO_4)_9$, ($x \approx 0.11$) [54], and a similar splitting of the K/Ag position was found by us in the structure of $Ag_{1.32}K_{6.68}(MoO_4)_4$ [50]. Such disordering and splitting of positions of large alkali cations is still rare. Examples are rubidium-containing defect pyrochlores $RbNb_2O_5F$ [55], $RbAl_{0.33}W_{1.67}O_6$ [56], ferroelectric solid electrolytes $RbTiOAsO_4$ [57] and $RbSbOGeO_4$ [58] of the $KTiOPO_4$ type. As a rule, this is considered as the ability of the structure to have potential ionic conductivity and/or ferroelectricity [59]. Indeed, some rubidium-containing defect pyrochlores and many members of the $KTiOPO_4$ family are bright examples of phases with these properties [58, 60]. This tendency is confirmed by the fact that the $Ag_{3+x}Rb_{9-x}Sc_2(WO_4)_9$ ($x \approx 0.11$) studied by us probably has rubidium ion conductivity [54], and nonstoichiometric phases of the glaserite type can also be solid electrolytes [61].

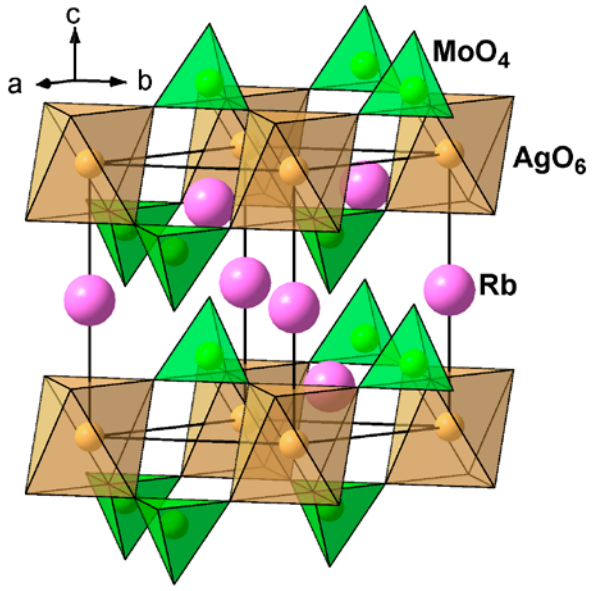

Fig. 2. General view of the $Rb_{2.81}Ag_{1.19}(MoO_4)_2$ structure

3.3. Crystal structure of $Tl_{3.14}Ag_{0.86}(MoO_4)_2$

According to [47, 48], in the Tl_2MoO_4–Ag_2MoO_4 system, boundary solid solutions are formed, including those based on the high-temperature hexagonal form α-Tl_2MoO_4 of the $K_3Na(SO_4)_2$ glaserite type [51]. Using spontaneous crystallisation of a molten sample of $Tl_3Ag(MoO_4)_2$ synthesized by solid-state reactions from a stoichiometric mixture of simple molybdates, we obtained crystals suitable for X-ray structural analysis from the region of the specified solid solution and refined their crystal structure.

The composition of the studied crystal of the glaserite type, $Tl_{3.14}Ag_{0.86}(MoO_4)_2$ (sp. gr. $P\bar{3}m1$), was determined by refinement of the site occupancies of the thallium and silver cations, which showed that the occupancy of thallium sites is 100 % within the experimental error limits, while the silver site contains an admixture of thallium. The correctness of this model is confirmed by a decrease in *R*-factor from 0.0235 to 0.0174, and the determined crystal composition fell into the range of the solid solution based on α-Tl_2MoO_4. The results of the structural refinement are given in Table 4, and the atomic coordinates and interatomic distances are shown in Tables 7 and 8.

In general, the structure of $Tl_{3.14}Ag_{0.86}(MoO_4)_2$ repeats the above-described structure of isostructural $Rb_{2.81}Ag_{1.19}(MoO_4)_2$ (Fig. 2). Molybdenum atoms are tetrahedrally coordinated with the distances Mo–O 1.760 (6)–1.765(3) Å, and the (Ag, Tl) atom has octahedral coordination with equal bond lengths (Ag, Tl)–O 2.535(4) Å, which is longer than the distance Ag1–O 2.483(3) Å in $Rb_{2.81}Ag_{1.19}(MoO_4)_2$ (see above) and is significantly shorter than the corresponding distance Tl1–O 2.769(10) Å in the structure of α-Tl_2MoO_4 [51]. Thallium atoms of two sorts with CN = 12 and 10 have the common distance range Tl–O 2.495(7)–3.5243(4) Å, which is close to the lengths of the corresponding bonds Tl–O 2.467(16)–3.682(16) Å in α-Tl_2MoO_4 [51].

4. Conclusions

The subsolidus region of the system Ag_2MoO_4–Cs_2MoO_4 was studied by PXRD, the compound with the composition $CsAg_3(MoO_4)_2$ crystallising in the structure type of $Ag_2BaMn(VO_4)_2$ (sp. gr. $P\bar{3}$, Z = 1) was revealed and its structure was determined.

Table 7. Coordinates and equivalent isotropic thermal parameters of atoms in the structure of $Tl_{3.14}Ag_{0.86}(MoO_4)_2$

Atom	Occ.	*x/a*	*y/b*	*z/c*	U_{eq} (Å²)*
Mo	1	0.6667	0.3333	0.29677(10)	0.0195(2)
(Ag, Tl)	0.877(5)Ag+0.123Tl	0	0	0	0.0282(3)
Tl1	1	0.3333	0.6667	0.16186(4)	0.0328(2)
Tl2	1	0	0	0.5	0.0316(2)
O1	1	0.6667	0.3333	0.5207(10)	0.062(3)
O2	1	0.8232(4)	0.6464(7)	0.2181(6)	0.0399(10)

*$U_{eq} = 4(U_{11} + U_{22} + 0.75U_{33} - U_{12}) / 9$.

Table 8. Main interatomic distances (Å) in the structure of $Tl_{3.14}Ag_{0.86}(MoO_4)_2$

Mo-tetrahedron		Tl1-polyhedron	
Mo–O1	1.760(8)	Tl1–O1	2.495(7)
–O2	1.765(4) × 3	–O2	3.0825(7) × 6
		–O2′	3.413(4) × 3
<Mo–O>	1.764	<Tl1–O>	3.123
(Ag, Tl)-octahedron		Tl2-polyhedron	
(Ag, Tl)–O2	2.535(4) × 6	Tl2–O2	2.898(4) × 6
		–O1	3.5243(4) × 6
		<Tl2–O>	3.211

We determined the structure and composition of double rubidium-silver molybdate, and performed X-ray structure analysis of a member of the solid solution on the base of the high-temperature form of thallium molybdate formed in the system Ag_2MoO_4–Tl_2MoO_4. It was confirmed that $Rb_{2.81}Ag_{1.19}(MoO_4)_2$ and $Tl_{3.14}Ag_{0.86}(MoO_4)_2$ (crystal compositions were determined by X-ray structure analysis) are of the glaserite structure type. In the case of the rubidium containing phase, splitting of the Rb/Ag position was revealed for the first time in molybdates. This phenomenon usually indicates the ability of the structure to have potential ionic conductivity and/or ferroelectricity.

Author contributions

All authors made an equivalent contribution to the preparation of the publication.

Conflict of interests

The authors declare that they have no known competing financial interests or personal relationships that could have influenced the work reported in this paper.

References

1. Fan W., He Y., Long L., Gao Y., Liu F., Liu J. Multiplexed excitations $KGd_{1-x}Eu_x(MoO_4)_2$ red-emitting phosphors with highly Eu^{3+} doping for white LED application. *Journal of Materials Science: Materials in Electronics*. 2021;32(5): 6239–6248. https://doi.org/10.1007/s10854-021-05339-1

2. Wang Y., Song M., Xiao L., Li Q. Upconversion luminescence of Eu^{3+} and Sm^{3+} single-doped $NaYF_4$ and $NaY(MoO_4)_2$. *Journal of Luminescence*. 2021;238: 118203. https://doi.org/10.1016/j.jlumin.2021.118203

3. Morozov V. A., Lazoryak B. I., Shmurak S. Z., Kiselev A. P., Lebedev O. I., Gauquelin N., Verbeeck J., Hadermann J., Van Tendeloo G. Influence of the structure on the properties of $Na_xEu_y(MoO_4)_z$ red phosphors. *Chemistry of Materials*. 2014;26(10): 3238–3248. https://doi.org/10.1021/cm500966g

4. Guo C., Gao F., Xu Y., Liang L., Shi F. G., Yan B. Efficient red phosphors $Na_5Ln(MoO_4)_4$: Eu^{3+} (*Ln* = La, Gd and Y) for white LEDs. *Journal of Physics D: Applied Physics*. 2009;42(9): 095407. https://doi.org/10.1088/0022-3727/42/9/095407

5. Zhao C., Yin X., Huang F., Hang Y. Synthesis and photoluminescence properties of the high-brightness Eu^{3+}-doped $M_2Gd_4(MoO_4)_7$ (*M* = Li, Na) red phosphors. *Journal of Solid State Chemistry*. 2011;184(12): 3190–3194. https://doi.org/10.1016/j.jssc.2011.09.025

6. Pandey I. R., Karki S., Daniel D. J., Kim H. J., Kim Y. D., Lee M. H., Pavlyuk A. A., Trifonov V. A. Crystal growth, optical, luminescence and scintillation characterization of $Li_2Zn_2(MoO_4)_3$ crystal. *Journal of Alloys and Compounds*. 2021;1860: 158510. https://doi.org/10.1016/j.jallcom.2020.158510 0925-8388

7. Isupov V. A. Binary molybdates and tungstates of mono and trivalent elements as possible ferroelastics and ferroelectrics. *Ferroelectrics*. 2005;321(1): 63–90. https://doi.org/10.1080/00150190500259699

8. Isupov V. A. Ferroelectric and ferroelastic phase transitions in molybdates and tungstates of monovalent and bivalent elements. *Ferroelectrics*. 2005;322(1): 83–114. https://doi.org/10.1080/00150190500315574

9. Tsyrenova G. D., Pavlova E. T., Solodovnikov S. F., Popova N. N., Kardash T. Yu., Stefanovich S. Yu., Gudkova I. A., Solodovnikova Z. A., Lazoryak B. I. New ferroelastic $K_2Sr(MoO_4)_2$: synthesis, phase transitions, crystal and domain structures, ionic conductivity. *Journal of Solid State Chemistry*. 2016;237: 64–71. https://doi.org/10.1016/j.jssc.2016.01.011

10. Savina A. A., Solodovnikov S. F., Basovich O. M., Solodovnikova Z. A., Belov D. A., Pokholok K. V., Gudkova I. A., Stefanovich S. Yu., Lazoryak B. I., Khaikina E. G. New double molybdate $Na_9Fe(MoO_4)_6$: synthesis, structure, properties. *Journal of Solid State Chemistry*. 2013;205: 149–153. https://doi.org/10.1016/j.jssc.2013.07.007

11. Savina A. A., Morozov V. A., Buzlukov A. L., Arapova I. Yu., Stefanovich S. Yu., Baklanova Ya. V., Denisova T. A., Medvedeva N. I., Bardet M., Hadermann J., Lazoryak B. I., Khaikina E. G. New solid electrolyte $Na_9Al(MoO_4)_6$: structure and Na^+ ion conductivity. *Chemistry of Materials*. 2017;29(20): 8901–8913. https://doi.org/10.1021/acs.chemmater.7b03989

12. Solodovnikov S. F., Solodovnikova Z. A., Zolotova E. S., Yudin V. N., Gulyaeva O. A., Tushinova Y. L., Kuchumov B. M. Nonstoichiometry in the systems Na_2MoO_4–$MMoO_4$ (*M* = Co, Cd), crystal structures of $Na_{3.36}Co_{1.32}(MoO_4)_3$, $Na_{3.13}Mn_{1.43}(MoO_4)_3$ and $Na_{3.72}Cd_{1.14}(MoO_4)_3$, crystal chemistry, compositions and ionic conductivity of alluaudite-type double molybdates and tungstates. *Journal of Solid State Chemistry*. 2017;253: 121–128. https://doi.org/10.1016/j.jssc.2017.05.031

13. Medvedeva N. I., Buzlukov A. L., Skachkov A. V., Savina A. A., Morozov V. A., Baklanova Ya. V., Animitsa I. E., Khaikina E. G., Denisova T. A., Solodovnikov S. F. Mechanism of sodium-ion diffusion in alluaudite-type $Na_5Sc(MoO_4)_4$ from NMR experiment and ab initio calculations. *Journal of Physical Chemistry C*. 2019;123(8): 4729. https://doi.org/10.1021/acs.jpcc.8b11654

14. Chen S., Duan H., Zhou Z., Fan Q., Zhao Y., Dong Y. Lithiated bimetallic oxide, $Li_3Fe(MoO_4)_3$, as a high-performance anode material for lithium-ion batteries and its multielectron reaction mechanism. *Journal of Power Sources*. 2020;476: 228656. https://doi.org/10.1016/j.jpowsour.2020.228656

15. Tamboli A. M., Tamboli M. S., Praveen C. S., Dwivedi P. K., Karbhal I., Gosavi S. W., Shelke M. V., Kale B. B. Architecture of $NaFe(MoO_4)_2$ as a novel anode material for rechargeable lithium and sodium ion batteries. *Applied Surface Science*. 2021;559: 149903. https://doi.org/10.1016/j.apsusc.2021.149903

16. Wang L., He Y., Mu Y., Wu B., Liu M., Zhao Y., Lai X., Bi J., Gao D. Sol-gel driving $LiFe(MoO_4)_2$ microcrystals: high capacity and superior cycling stability for anode material in lithium ion batteries. *Electronic Materials Letters*. 2019;15(2): 186–191. https://doi.org/10.1007/s13391-018-00115-6

17. Mikhailova D., Sarapulova A., Voss A., Thomas A., Oswald S., Gruner W., Trots D. M., Bramnik N. N., Ehrenberg H. $Li_3V(MoO_4)_3$: A new material for both Li extraction and insertion. *Chemistry of Materials*. 2010;22(10): 3165–3173. https://doi.org/10.1021/cm100213a

18. Begam K. M., Prabaharan S. R. S. Improved cycling performance of nano-composite $Li_2Ni_2(MoO_4)_3$ as a lithium battery cathode material. *Journal of Power Sources*. 2006;159(1): 319–322. https://doi.org/10.1016/j.jpowsour.2006.04.133

19. Serdtsev A. V., Medvedeva N. I. Ab initio insights into Na-ion diffusion and intercalation mechanism in alluaudite $Na_2Mn_2(MoO_4)_3$ as cathode material for sodium-ion batteries. *Journal of Alloys and Compounds*. 2019;808: 151667. https://doi.org/10.1016/j.jallcom.2019.151667

20. Voron'ko Yu. K., Zharikov E. V., Lis D. A., Popov A. V., Smirnov V. A., Subbotin K. A., Khromov M. N., Voronov V. V. Growth and spectroscopic studies of $NaLa(MoO_4)_2$:Tm^{3+} crystals: a new promising laser material. *Optics and Spectroscopy*. 2008;105(4): 538–546. https://doi.org/10.1134/S0030400X08100081

21. Gao S., Zhu Z., Wang Y., You Z., Li J., Wang H., Tu C. Growth and spectroscopic investigations of a new laser crystal Yb^{3+}-doped $Na_2Gd_4(MoO_4)_7$. *Optical Materials*. 2013;36(2): 505–508. https://doi.org/10.1016/j.optmat.2013.10.018

22. Loiko P., Pavlyuk A., Slimi S., Solé R. M., Salem E. B., Dunina E., Kornienko A., Camy P., Griebner U., Petrov V., Díaz F., Aguiló M., Mateos X. Growth, spectroscopy and laser operation of monoclinic Nd:$CsGd(MoO_4)_2$ crystal with a layered structure. *Journal of Luminescence*. 2021;231: 117793. https://doi.org/10.1016/j.jlumin.2020.117793

23. Iparraguirre I., Balda R., Voda M., Al-Saleh M., Fernandez J. Infrared-to-visible upconversion in $K_5Nd(MoO_4)_4$ stoichiometric laser crystal. *Journal of the Optical Society of America B*. 2002;19(12): 2911–2920. https://doi.org/10.1364/JOSAB.19.002911

24. Voron'ko Y. K., Subbotin K. A., Shukshin V. E., Lis D. A., Ushakov S. N., Popov A., Zharikov E. V. Growth and spectroscopic investigations of Yb^{3+}-doped $NaGd(MoO_4)_2$ and $NaLa(MoO_4)_2$: new promising laser crystals. *Optical Materials*. 2006;29(2-3): 246–252. https://doi.org/10.1016/j.optmat.2005.09.004

25. Hoermann F. Beitrag zur Kenntnis der Molybdate und Wolframate. Die binären Systeme: Li_2MoO_4–MoO_3, Na_2MoO_4–MoO_3, K_2MoO_4–MoO_3, Li_2WO_4–WO_3, Na_2WO_4–WO_3, K_2WO_4–WO_3, Li_2MoO_4–Na_2MoO_4, Li_2WO_4–Na_2WO_4, Li_2MoO_4–K_2MoO_4. *Zeitschrift für Anorganische und Allgemeine Chemie*. 1929;177(1): 145–186. https://doi.org/10.1002/zaac.19291770117

26. Bergman A. G., Kislova A. I., Korobka E. I. Issledovanie dvoinoi vzaimnoi sistemy diagonal'no-poyasnogo tipa iz sul'fatov i molibdatov litiya i kaliya [Investigation of the double reciprocal system of the diagonal-belt type of lithium and potassium sulfates and molybdates]. *Zhurnal Obshhej Khimii*. 1954;24(5): 1127–1135. (In Russ.)

27. Samuseva R. G., Bobkova M. V., Plyushchev V. E. Systems Li_2MoO_4–Rb_2MoO_4 and Li_2MoO_4–Cs_2MoO_4. *Zhurnal Neorganicheskoj Khimii (Russian Journal of Inorganic Chemistry*. 1969;14(11): 3140–3142. (In Russ.)

28. Klevtsova R. F., Klevtsov P. V., Aleksandrov K. S. Synthesis and crystal structure of $CsLiMoO_4$. *Doklady AN SSSR*. 1980;255(6): 1379–1382. Available at: http://www.mathnet.ru/links/615f6831862802e4f119568c63999bbe/ dan44135.pdf (In Russ.)

29. Okada K., Ossaka J. Crystal data and phase transitions of $KLiWO_4$ and $KLiMoO_4$. *Journal of Solid State Chemistry*. 1981;37(3): 325–327. https://doi.org/10.1016/0022-4596(81)90494-1

30. Aleksandrov K. S., Anistratov A. T., Melnikova S. V., Klevtsova P. F. Ferroelectricity in caesium lithium molybdate $CsLiMoO_4$ and related crystals $CsLiWO_4$ and $RbLiMoO_4$. *Ferroelectrics*. 1981;36(1): 399–402. https://doi.org/10.1080/00150198108218138

31. Kruglik A. I., Klevtsova P. F., Aleksandrov K. S. Crystal structure of new ferroelectric $RbLiMoO_4$. *Doklady AN SSSR*. 1983;271(6): 1388–1391. Available at: http://www.mathnet.ru/links/b19a6f8fab3efdda809632d278dc8cb9/dan46252.pdf (In Russ.)

32. Melnikova S. V., Voronov V. N., Klevtsov P. V. Phase transitions in $RbLiMoO_4$. *Kristallografiya*. 1986;31(2): 402–404. (In Russ.)

33. Ding Y., Hou N., Chen N., Xia Y. Phase diagrams of Li_2MoO_4–Na_2MoO_4 and Na_2MoO_4–K_2MoO_4 systems. *Rare metals*. 2006;25(4): 316–320. https://doi.org/10.1016/S1001-0521(06)60060-0

34. Bergman A. G., Korobka E. I. Fusibility diagram of a ternary reciprocal system of lithium and sodium sulfates and molybdates. *Zhurnal Neorganicheskoj Khimii (Russian Journal of Inorganic Chemistry)*. 1959;4(1): 110–116. (In Russ.)

35. Fabry J., Petricek V., Vanek P., Cisarova I. Phase transition in $K_3Na(MoO_4)_2$ and determination of the twinned structures of $K_3Na(MoO_4)_2$ and $K_{2.5}Na_{1.5}(MoO_4)_2$ at room temperature. *Acta Crystallographica Section B*. 1997;53(4): 596–603. https://doi.org/10.1107/s0108768197002164

36. Gulyaeva O. A., Solodovnikova Z. A., Solodovnikov S. F., Yudin V. N., Zolotova E. S., Komarov V. Yu. Subsolidus phase relations and structures of solid solutions in the systems K_2MoO_4–Na_2MoO_4–$MMoO_4$ (M = Mn, Zn). *Journal of Solid State Chemistry*. 2019;272: 148–156. https://doi.org/10.1016/j.jssc.2019.02.010

37. Mokhosoev M. V., Khal'baeva K. M., Khaikina E. G., Ogurtsov A. M. Double sodium-rubidium molybdates. *Zhurnal Neorganicheskoj Khimii (Russian Journal of Inorganic Chemistry)*. 1990;35(8): 2126–2129. Available at: https://elibrary.ru/item.asp?id=22232925 (In Russ.)

38. Bai C., Lei C., Pan S., Wang Y., Yang Z., Han S., Yu H., Yang Y., Zhang F. Syntheses, structures and characterizations of $Rb_3Na(MO_4)_2$ (M = Mo, W) crystals. *Solid State Science*. 2014;33: 32–37. https://doi.org/10.1016/j.solidstatesciences.2014.04.011

39. Zolotova E. S., Solodovnikova Z. A., Yudin V. N., Solodovnikov S. F., Khaikina E. G., Basovich O. M., Korolkov I. V., Filatova I. Yu. Phase relations in the Na_2MoO_4–Cs_2MoO_4 and Na_2MoO_4–Cs_2MoO_4–$ZnMoO_4$ systems, crystal structures of $Cs_3Na(MoO_4)_2$ and $Cs_3NaZn_2(MoO_4)_4$. *Journal of Solid State Chemistry*. 2016;233: 23–29. https://doi.org/10.1016/j.jssc.2015.10.008

40. Okada K., Ossaka J. Structures of potassium sodium sulphate and tripotassium sodium disulphate. *Acta Crystallographica Section B*. 1980;36(4): 919–921. https://doi.org/10.1107/S0567740880004852

41. Belyaev I. N., Doroshenko S. S. Study of the interaction of sulfates and molybdates of lithium and silver in melts. *Zhurnal Neorganicheskoj Khimii (Russian Journal of Inorganic Chemistry)*. 1956;26(7): 1816–1820. (In Russ.)

42. Khal'baeva K. M., Khaikina E. G., Basovich O. M. Phase equilibria in lithium-silver(sodium)-bismuth molybdate systems. *Russian Journal of Inorganic Chemistry*. 2005;50(8): 1282–1284.

43. Belyaev I. N., Doroshenko A. K. Exchange decomposition in a reciprocal system of sodium and silver sulfates and molybdates in melts. *Zhurnal Obshhej Khimii*. 1954;24: 427–432. (In Russ.)

44. Zhou D., Li J., Pang L. X., Wang D. W., Reaney I. M. Novel water insoluble $(Na_xAg_{2-x})MoO_4$ ($0 \leqslant x \leqslant 2$) microwave dielectric ceramics with spinel structure sintered at 410 degrees. *Journal of Materials Chemistry. C*. 2017;5(24): 6086–6091. https://doi.org/10.1039/c7tc01718a

45. Rulmont A., Tarte P., Foumakoye G., Fransolet A.M., Choisnet J. The disordered spinel $NaAgMoO_4$ and its high-temperature, ordered orthorhombic polymorph. *Journal of Solid State Chemistry*. 1988;76(1): 18–25. https://doi.org/10.1016/0022-4596(88)90188-0

46. Zhou D., Pang L. X., Qi Z. M., Jin B. B., Yao X. Novel ultra-low temperature co-fired microwave dielectric ceramic at 400 degrees and its chemical compatibility with base metal. *Scientific Reports*. 2014;4(1): 5980. https://doi.org/10.1038/srep05980

47. Arkhincheeva S. I., Bazarova J. G., Munkueva S. D. Solid-phase interaction of thallium and silver molybdates (tungstates). *Vestnik BGU. Khimiya (BSU bulletin. Chemistry).* 2004;(1): 43–47. (In Russ.)

48. Grossman V. G., Bazarov B. G., Bazarova J. G. Phase formation in Tl_2MoO_4–Ag_2MoO_4 and Tl_2WO_4–Ag_2WO_4 systems. *Izvestia Vuzov. Prikladnaya Khimiya i Biotekhnologiya (Proceedings of Universitets. Applied Chemistry and Biotechnology)*. 2018;8(3): 142–147. https://doi.org/10.21285/2227-2925-2018-8-3-142-147 (In Russ.)

49. Kadyrova Yu. M., Solodovnikov S. F., Solodovnikova Z. A., Basovich O. M., Spiridonova T. S., Khaikina E. G. New silver-rubidium double molybdate. *Vestnik BGU (BSU bulletin. Chemistry. Physics)*. 2015;3: 21–25. (In Russ.)

50. Spiridonova T. S., Solodovnikov S. F., Savina A. A., Solodovnikova Z. A., Stefanovich S. Yu., Lazoryak B. I., Korolkov I. V., Khaikina E. G. Synthesis, crystal structures and properties of the new compounds $K_{7-x}Ag_{1+x}(XO_4)_4$ (X = Mo, W). *Acta Crystallographica Section C*. 2017;73(12): 1071–1077. https://doi.org/10.1107/s2053229617015674

51. Friese K., Madariaga G., Breczewski T. $T1_2MoO_4$ at 350 K. *Acta Crystallographica Section C*. 1999;55(11): 1753–1755. https://doi.org/10.1107/S0108270199008616

52. Sheldrick G. M. SHELX97, Release 97-2. – Göttingen, Germany: Univ. of Göttingen, 1997.

53. Rettich R., Müller-Buschbaum Hk., Zur Kristallchemie der Silber-Mangan-Oxovanadate $Ag_2BaMnV_2O_8$ und $(AgCa_2)Mn_2(VO_4)_3$. *Zeitschrift für Naturforschung*. 1998;53b: 291–295. Available at: https://zfn.mpdl.mpg.de/data/Reihe_B/53/ZNB-1998-53b-0291.pdf

54. Spiridonova T. S., Solodovnikov S. F., Savina A. A., Kadyrova Yu. M., Solodovnikova Z. A., Yudin V. N., Stefanovich S. Yu., Kotova I. Yu., Khaikina E. G., Komarov V. Yu. $Rb_{9-x}Ag_{3+x}Sc_2(WO_4)_9$: a new glaserite-related structure type, rubidium disorder, ionic conductivity. *Acta Crystallographica Section B*. 2020;76(1): 28–37. https://doi.org/10.1107/S2052520619015270

55. Fourquet J. L., Jacoboni C., de Pape R. Les pyrochlores $A^I_2X_6$: mise en evidence de l'occupation par le cation A^I de nouvelles positions cristallographiques dans le groupe d'espace $Fd3m$. *Materials Research Bulletin*. 1973;8(4): 393–404. https://doi.org/10.1016/0025-5408(73)90043-3

56. Thorogood G. J., Kennedy B. J., Peterson V. K., Elcombe M. M., Kearley G. J., Hanna J. V., Luca V. Anomalous lattice parameter increase in alkali earth aluminium substituted tungsten defect pyrochlores. *Journal of Solid State Chemistry*. 2009;182(3): 457–464. https://doi.org/10.1016/j.jssc.2008.11.014

57. Streltsov V. A., Nordborg J., Albertsson J. Synchrotron X-ray analysis of $RbTiOAsO_4$. *Acta Crystallographica Section B*. 2000;56(5): 785–792. https://doi.org/10.1107/S0108768100006285

58. Belokoneva E. L., Knight K. S., David W. I. F., Mill B. V. Structural phase transitions in germanate analogues of $KTiOPO_4$ investigated by high-resolution neutron powder diffraction. *Journal of Physics: Condensed Matter*. 1997;9(19): 3833–3851. https://doi.org/10.1088/0953-8984/9/19/005

59. Kalinin V. B., Golubev A. M. Splitting of cationic positions in crystal structures with special electrophysical properties. *Kristallografiya (Soviet Physics. Crystallography)*. 1990;35(6): 1472–1478. (In Russ.)

60. Astaf'ev A. V., Bosenko A. A., Voronkova V. I., Krasheninnikova M. A., Stefanovich S. Yu., Yanovskij V. K. Dielectric, optical properties and ionic conductivity of $TlNbWO_6$ and $RbNbWO_6$ crystals. *Kristallografiya (Soviet Physics. Crystallography)*. 1986;31(5): 968–973. (In Russ.)

61. Serdtsev A. V., Suetin D. V., Solodovnikov S. F., Gulyaeva O. A., Medvedeva N. I. Electronic structure and sodium-ion diffusion in glaserite-type $A_{3-x}Na_{1+x}(MoO_4)_2$ (A = Cs, K) studied with first-principles calculations. *Solid State Ionics*. 2020;357: 115484. https://doi.org/10.1016/j.ssi.2020.115484

Information about the authors

Tatiana S. Spiridonova, PhD in Chemistry, Researcher, Laboratory of Oxide Systems, Baikal Institute of Nature Management, Siberian Branch of the Russian Academy of Sciences (BINM SB RAS), Ulan-Ude, Russian Federation; e-mail: spiridonova-25@mail.ru. ORCID iD: https://orcid.org/0000-0001-7498-5103.

Sergey F. Solodovnikov, DSc in Chemistry, Professor, Leading Researcher, Laboratory of Crystal Chemistry, Nikolaev Institute of Inorganic Chemistry, Siberian Branch of the Russian Academy of Sciences (NIIC SB RAS), Novosibirsk, Russian Federation; e-mail: solod@niic.nsc.ru. ORCID iD: https://orcid.org/0000-0001-8602-5388.

Yulia M. Kadyrova, PhD in Chemistry, Researcher, Laboratory of Oxide Systems, Baikal Institute of Nature Management, Siberian Branch of the Russian Academy of Sciences (BINM SB RAS) and Senior Lecturer of the Department of General and Analytical Chemistry, Faculty of Chemistry, Banzarov Buryat State University (BSU), Ulan-Ude, Russian Federation; e-mail: yliychem@yandex.ru. ORCID iD: https://orcid.org/0000-0002-0106-8096.

Zoya A. Solodovnikova, PhD in Chemistry, Researcher, Laboratory of Crystal Chemistry, Nikolaev Institute of Inorganic Chemistry, Siberian Branch of the Russian Academy of Sciences (NIIC SB RAS), Novosibirsk, Russian Federation; e-mail: zoya@niic.nsc.ru. ORCID iD: https://orcid.org/0000-0001-5335-5567.

Alexandra A. Savina, PhD in Chemistry, Senior Researcher, Laboratory of Oxide Systems, Baikal Institute of Nature Management, Siberian Branch of the Russian Academy of Sciences (BINM SB RAS), Ulan-Ude, Russian Federation and Researcher, Skolkovo Institute of Science and Technology, Moscow, Russian Federation, e-mail: a.savina@skoltech.ru. ORCID iD: https://orcid.org/0000-0002-7108-8535.

Elena G. Khaikina, DSc in Chemistry, Professor, Chief Researcher, Laboratory Oxide Systems, Baikal Institute of Nature Management, Siberian Branch of the Russian Academy of Sciences (BINM SB RAS) and Professor of the Department of Inorganic and Organic Chemistry, Faculty of Chemistry, Banzarov Buryat State University (BSU), Ulan-Ude, Russian Federation; e-mail: egkha@mail.ru. ORCID iD: https://orcid.org/0000-0003-2482-9297.

Received 20 June 2021; Approved after reviewing 28 June 2021; Accepted for publication 15 July 2021; Published online 25 September 2021.

Translated by Valentina Mittova
Edited and proofread by Simon Cox